

*Short note***Ground-state spin of  $^{59}\text{Mn}$** 

M. Oinonen<sup>1,a</sup>, U. Köster<sup>1</sup>, J. Äystö<sup>1</sup>, V. Fedoseyev<sup>2</sup>, V. Mishin<sup>2</sup>, J. Huikari<sup>3</sup>, A. Jokinen<sup>3</sup>, A. Nieminen<sup>3</sup>, K. Peräjärvi<sup>3</sup>, A. Knipper<sup>4</sup>, and G. Walter<sup>4</sup>  
 the ISOLDE Collaboration

<sup>1</sup> EP Division, CERN, CH-1211 Geneva 23, Switzerland

<sup>2</sup> Institute of Spectroscopy, Russian Academy of Sciences, RU-142092 Troitsk, Russia

<sup>3</sup> Department of Physics, University of Jyväskylä, FIN-40351 Jyväskylä, Finland

<sup>4</sup> Institut de Recherches Subatomiques, F-67037 Strasbourg Cedex 2, France

Received: 17 November 2000 / Revised version: 6 February 2001

Communicated by D. Guereau

**Abstract.** Beta-decay of  $^{59}\text{Mn}$  has been studied at PSB-ISOLDE, CERN. The intense and pure Mn beam was produced using the Resonance Ionization Laser Ion Source (RILIS). Based on the measured  $\beta$ -decay rates the ground-state spin and parity are proposed to be  $J^\pi = 5/2^-$ . This result is consistent with the systematic trend of the odd- $A$  Mn nuclei and extends the systematics one step further towards the neutron drip line.

**PACS.** 21.10.-k Properties of nuclei; nuclear energy levels – 23.40.-s Beta decay – 27.50.+e  $59 \leq A \leq 89$

**1 Introduction**

Among the most fundamental properties that can be experimentally determined for a given nucleus are ground-state spin and parity. Systematical studies of nuclei over large range in proton and neutron numbers give information on the nature of the states ranging from single-particle to the strongly-mixed collective ones. In addition, the knowledge of the ground-state spin lays necessary foundation for detailed studies of nuclear level structure.

Along the isotopic chain of Mn nuclei the ground-state spin and parity have been determined firmly from  $^{48}\text{Mn}$  up to  $^{58}\text{Mn}$ . The low-lying level structure in the odd-even Mn nuclei is characterized by a  $5/2^-$ - $7/2^-$  doublet. In a framework of the extreme single-particle shell model the  $7/2^-$  state is due to the 25th proton which is in the  $1f_{7/2}$  subshell. Nature of the low-energy levels in the odd- $A$  Mn isotopes between  $^{53-57}\text{Mn}$  has been studied by Puttaswamy *et al.*, [1]. Indeed, the  $7/2^-$  state was found to have a strong single-particle nature unlike the other states including the  $5/2^-$  level which possesses a very strong collective character. Nucleon-nucleon interaction forces the state with  $J^\pi = 5/2^-$  to be the ground state for all the odd-even Mn isotopes between  $A = 49$  and  $57$  except for  $^{53}\text{Mn}$ . The closed neutron shell with  $N = 28$  in the case of  $^{53}\text{Mn}$  leaves a possibility for the odd proton to define the ground state as  $J^\pi = 7/2^-$ .

Using the heavy-ion fusion evaporation reaction  $^{48}\text{Ca}(^{13}\text{C}, \text{pn})^{59}\text{Mn}$ , Pardo *et al.*, [2] were able to detect allowed  $\beta$  transitions to the lowest five excited states in  $^{59}\text{Fe}$ . However, due to the fact that the branching ratio for the transition to the ground state in  $^{59}\text{Fe}$  could not be determined, only lower limits for the  $\log ft$  values for the individual transitions could be set. Therefore, the question of the spin of the ground state of  $^{59}\text{Mn}$  was left unsolved in that work but was restricted to be  $3/2^-$  or  $5/2^-$  [2]. In addition, the experimental probes such as the  $^{64}\text{Ni}(^3\text{He}, ^8\text{B})$  reaction [3], the  $\beta$ -decay of  $^{59}\text{Cr}$  [4] and the  $^{59}\text{Co}(\pi^-, \pi^+)$  reaction [5] have been used in studies of  $^{59}\text{Mn}$ . Information obtained on the low-lying levels have been restricted to the mass excess of the ground state [3] and to the observation of two excited states at  $\sim 1.3$  MeV [4]. Knowledge of the level structure of the daughter nucleus  $^{59}\text{Fe}$  has been later on improved by the  $^{58}\text{Fe}(\text{d}, \text{p})$  [6] and  $^{58}\text{Fe}(\text{n}, \gamma)$  [7] reaction studies. In addition, recently a Coulomb excitation study on the secondary  $^{59}\text{Mn}$  beam was performed at NSCL using fragmentation of  $^{64}\text{Ni}$ [8] but the analysis suffers from the uncertainty of the ground-state  $J^\pi$  of  $^{59}\text{Mn}$ .

An experiment on the  $\beta$ -decay of  $^{59}\text{Mn}$  was performed at the ISOLDE on-line mass separator facility at CERN using the Resonance Ionization Laser Ion Source (RILIS). A high yield of  $2 \times 10^6$  at/ $\mu\text{C}$  for  $^{59}\text{Mn}$  obtained made possible a high-precision half-life measurement and determination of  $\beta$ -decay feedings, particularly to the ground state of  $^{59}\text{Fe}$ . In this paper we report on these mea-

<sup>a</sup> e-mail: Markku.Oinonen@cern.ch

measurements for determining the ground-state spin of  $^{59}\text{Mn}$  based on the  $\beta$ -decay transition rates observed.

## 2 Experimental methods

Mn nuclei were produced in spallation reactions in a 50 g/cm<sup>2</sup> thick Nb-foil target induced by 1 GeV pulsed proton beam from PS-Booster at CERN. In general, the PS-Booster provides 12 pulses of intensity of  $3 \times 10^{13}$  protons/pulse within 14.4 s supercycle. The distance between the successive pulses is 1.2 s. During the experiment typically 7–8 pulses of these within one supercycle were taken into the ISOLDE target. After ionization the extracted ions were mass separated in the General Purpose Separator (GPS) and implanted into a movable implantation tape surrounded by the detection setup described below.

The laser ion source at ISOLDE is based on the method of resonant laser ionization in a hot cavity. Detailed description of the RILIS concept used at ISOLDE has been given in [9]. In short, the ionization occurs inside a hot capillary tube where the laser light is guided through a quartz window in the vacuum chamber of the separator magnet. Mechanical and chemical stability reasons limit the material of the capillary to refractory elements such as Ta, W or Nb. The capillary is kept hot, typically in 2200 K, to prevent sticking of the produced atoms at the walls of the tube. Thus, the wall acts as a surface ionizer and reduces the selectivity of the LIS due to ionisation of the elements with low ionisation potentials. On the other hand, this surface ionization character allows the target to be used more effectively and even in the absence of laser ionization. Excitation schemes for Mn isotopes have been studied by Fedoseyev *et al.* [10]. In this work we used the scheme shown in fig. 1. This scheme was found to have the best relative ionization efficiency. This is due to capability of the third-step transition to resonantly excite the autoionizing state above the ionization potential of 7.44 eV. The yields observed for Mn nuclei during the experiment have been reported in [11].

The measurement set-up was placed in a close geometry around the implantation position and consisted of a  $\beta$  telescope and a coaxial Ge detector with relative efficiency of 70% for  $\gamma$ -ray detection. The  $\beta$  telescope was a combination of a thin 2-mm-thick scintillator, which provided the trigger signal for the event, and a 20-mm-thick planar Ge detector. Two energy signals with different amplifications were taken out from the planar detector. A low-gain signal was used for high-energy  $\beta$  detection and a high-gain signal to search for low-energy  $\gamma$ -rays. Data were collected in list-mode by using the GOOSY acquisition system. In addition,  $\beta$ -gated  $\gamma$ -spectra and  $\beta$ -multiscaling spectra were collected with the SAM acquisition system from IReS, Strasbourg. The  $\gamma$ -intensities were measured with the coaxial Ge detector. The relative efficiency calibration for this detector was obtained using the sources of  $^{50\text{m}}\text{Mn}$ ,  $^{57}\text{Mn}$  and  $^{74}\text{Ga}$  collected online. The detection efficiency for the  $\gamma$ -rays in coincidence with the  $\beta$ -particles was determined using the well-known decay of  $^{47}\text{K}$ . The

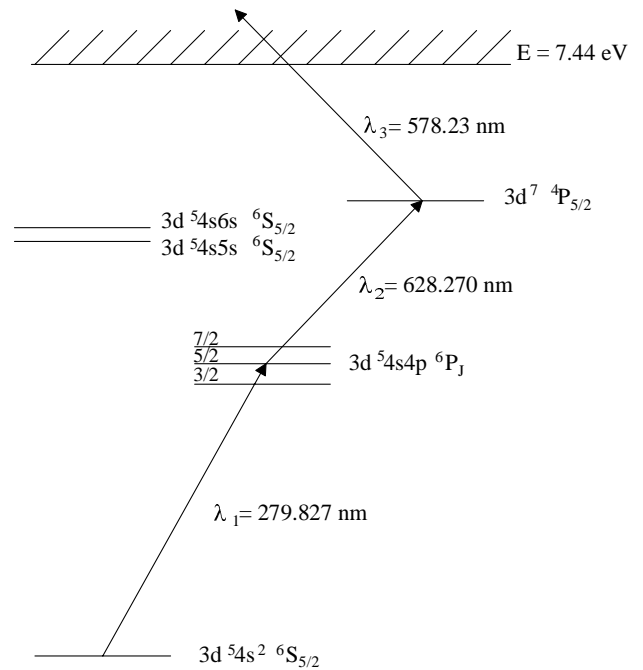


**Fig. 1.** Laser ionization scheme used in this work for Mn.

largest uncertainty was induced by the counting statistics in  $\beta$  and  $\beta$ -gated  $\gamma$  spectra.

Two runs were performed for  $^{59}\text{Mn}$ , the first one with the maximum number of proton pulses available to maximize the counting statistics for the  $\gamma$ -ray intensities. The second run was made with only one pulse per supercycle of the PS-Booster (14.4 s) with a short collection period of 50 ms. The latter run had two aims: to minimize dead-time and to have a long decay period for half-life analysis within the 14.4 s supercycle. The implantation tape was moved after every 20th pulse.

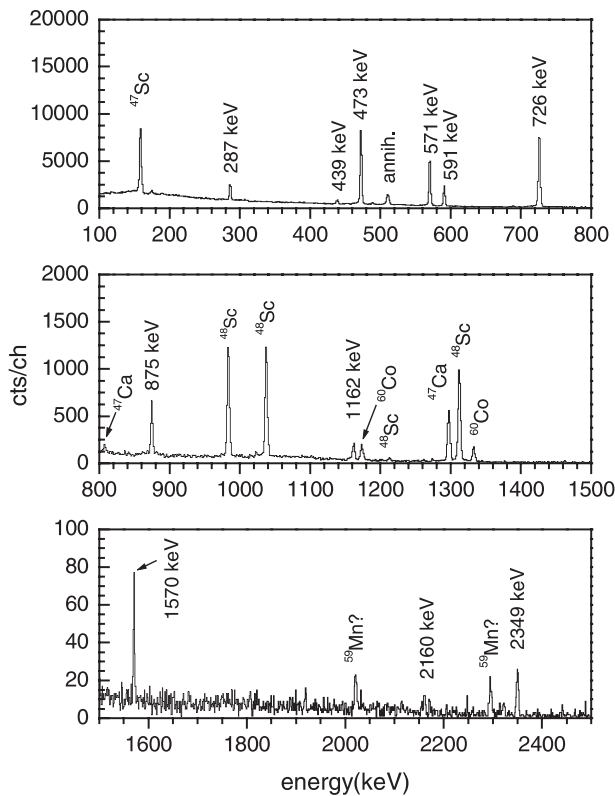
## 3 Results

The half-life of  $^{59}\text{Mn}$  was determined from the  $\beta$ -decay rate measured with the thin scintillator and the multiscaling acquisition system. Single exponential curve with a constant background was fitted into the multiscaling spectrum of  $\beta$ -rays. The new value obtained is  $T_{1/2} = 4.59(5)$  s. Agreement with the previous value of  $T_{1/2} = 4.6(1)$  s [2] is excellent.

The total number of  $\beta$  particles due to  $^{59}\text{Mn}$  decay was deduced from the listmode data collected with the multi-parameter system (GOOSY). First, the time spectrum of the  $\beta$  particles was fitted with a single exponential plus a constant background. The half-life of  $^{59}\text{Mn}$  was fixed to the new value given above. Then, the amount of background given by the constant was subtracted from the total number of counts to obtain the number of  $\beta$  particles due to  $^{59}\text{Mn}$  decay. The assumption of a constant background is justified since all the background activities observed have half-lives longer than 40 hours:  $^{48}\text{Sc}$ ,  $^{47}\text{Sc}$ ,

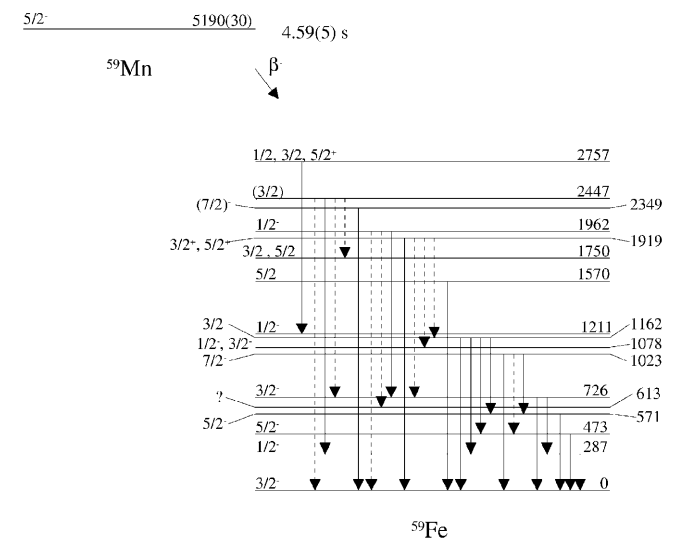
**Table 1.** Gamma-ray intensities measured in this work following the  $\beta$ -decay of  $^{59}\text{Mn}$ .

$E(\text{keV})^a$	$E(\text{keV})^b$	$E_{\text{adopted}}(\text{keV})$	Transition	$I_\gamma(\text{rel})$
287.03(13)	287.02(2)	287.02(2)	287→g.s.	11.0(11)
439.22(16)	439.43(4)	439.42(4)	726→287	3.7(5)
452.8(11)	452.32(11)	452.33(11)	1023→571	0.38(25)
472.74(15)	472.71(9)	472.72(8)	473→g.s.	68(7)
570.76(16)	570.81(5)	570.81(5)	571→g.s.	53(6)
591.1(3)	591.20(3)	591.20(3)	1162→571	22(3)
689.2(3)	688.6(5)	689.08(23)	1162→473	0.81(17)
726.30(17)	726.7(3)	726.40(15)	726→g.s.	100(10)
874.82(19)	875.12(5)	875.10(5)	1162→287	6.9(8)
1023.0(4)	1023.07(17)	1023.06(16)	1023→g.s.	0.21(16)
1161.7(3)	1162.17(8)	1162.12(8)	1162→g.s.	3.6(5)
1235	1235.54(4)	1235.54(4)	1962→726	<0.05
1545	1544.8(9)	1544.8(9)	2757→1211	<0.08
1569.4(7)	1569.88(8)	1569.87(8)	1570→g.s.	1.13(18)
1918.2(8)	1918.71(8)	1918.71(8)	1919→g.s.	0.21(6)
2159.9(10)	2160.20(6)	2160.20(6)	2447→287	0.37(9)
2348.9(9)	2345(10) <sup>c</sup>	2348.9(9)	2349 →g.s.	0.93(15)
total $\beta$ -intensity				316.6(5)

<sup>a</sup> This work.<sup>b</sup> Ref. [12].<sup>c</sup> Ref. [6].**Fig. 2.**  $\beta$ -delayed  $\gamma$  spectrum observed in the coaxial Ge detector.

$^{47}\text{Ca}$  resulting from the previous mass scans,  $^{60}\text{Co}$  and the daughter  $^{59}\text{Fe}$ .

Figure 2 shows the  $\beta$ -delayed  $\gamma$  spectrum observed in the coaxial Ge detector. List of the  $\gamma$  lines assigned to the

**Fig. 3.** Proposed decay scheme for  $^{59}\text{Mn}$ . The solid arrows correspond to the lines observed in this work. The dashed arrows are the transitions whose intensities have been taken from ref. [12]. See the text for more details.

decay of  $^{59}\text{Mn}$  is given in table 1. Assignments were based on the previously known level scheme of  $^{59}\text{Fe}$ . Altogether, we observed 16  $\gamma$ -rays compared to 9  $\gamma$ -rays reported in the previous work [2]. Other weak  $\gamma$  lines were also observed but these could not be assigned to any known activity. These were registered during the run for the maximum statistics and the time structure of the proton pulses was not suitable for half-life analysis. The strongest of these were the 191, 2020 and 2294 keV lines for which the rela-

**Table 2.** Beta-decay branching ratios and log  $ft$  values in the  $\beta$ -decay of  $^{59}\text{Mn}$ .

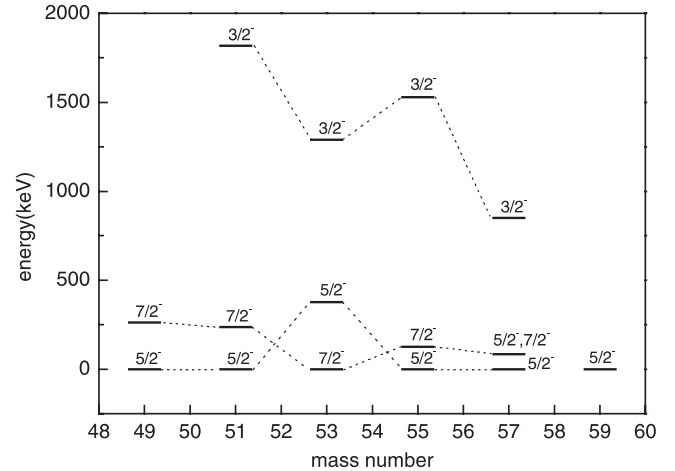
$E_f$ (keV)	$J_f^\pi$	$b(\%)$	$\log f^0t$	$\log f^1t$
0	$3/2^-$	25(5)	5.34(8)	
473	$5/2^-$	21.3(22)	5.21(5)	
571	$5/2^-$	9.8(19)	5.50(8)	
726	$3/2^-$	33(4)	4.91(4)	
1023	$7/2^-$	0.30(13)	6.81(19)	8.48(19)
1162	$3/2^-$	10.4(8)	5.19(4)	
1570	$5/2^-$	0.36(6)	6.43(7)	7.98(7)
1919	$3/2^+, 5/2^+$	0.09(2)	6.84(10)	8.30(10)
1962	$1/2^-$	<0.02	>7.4	>8.8
2349	$(7/2)^-$	0.29(5)	6.04(7)	7.38(8)
2447	$(3/2)$	0.19(4)	6.17(8)	7.48(8)
2757	$1/2^+, 3/2^+, 5/2^+$	<0.024	>6.8	>8.1

tive intensities varied between 0.7 and 1 %. However, these were most likely due to the beta-decay of  $^{59}\text{Mn}$  as well, since it was the only activity produced at  $A = 59$ .

Comparison of the  $\gamma$ -peak intensities and the total  $\beta$ -decay intensity lead to the decay scheme shown in fig. 3. The population of a certain level was determined as follows. The intensity of the strongest  $\gamma$  transition de-exciting the level in question was adopted from the present measurement. Relative intensities of the other transitions de-exciting the same level were adopted from the literature [12] and normalized using the strongest transition observed. Finally, the  $\beta$  feedings to the levels were obtained by using an intensity balance method. The branching ratios and the deduced log  $ft$  values are given in table 2.

## 4 Discussion

In the previous studies, the ground-state  $J^\pi$  of  $^{59}\text{Mn}$  has been deduced to be  $3/2^-$  or  $5/2^-$  [2,12]. In the present work, allowed beta transitions were observed to lead to the ground state and to the 473, 571, 726 and 1162 keV states in consistency with the previous spin/parity assignments. Our assignment for the ground-state spin/parity is based on the log  $ft$  values of transitions to the  $1/2^-$ - and  $7/2^-$ -states. If the ground-state spin were  $3/2$  there would be a possibility for allowed transitions to feed the known levels at 287, 1211 and 1962 keV that have  $J^\pi = 1/2^-$ . However, no feedings to these states were observed. As shown in table 1, feeding to the 287 keV level is zero within the experimental uncertainty. The 1211 keV peak was observed but completely explained by the decay of the contaminant  $^{48}\text{Sc}$ . Feeding of the 1962 keV state should be accompanied by a 1235 keV  $\gamma$  transition. However, no such a peak was observed. An upper limit of <0.02% can only be set for the  $\beta$ -decay branching ratio to this state corresponding to  $\log f^0t > 7.4$  and  $\log f^1t > 8.8$ . On the other hand, relatively strong transitions were observed to feed the states at 1023 keV and 2349 keV that have  $J^\pi$

**Fig. 4.** Level systematics of the odd- $A$  Mn isotopes from  $A = 51$  to  $A = 59$  showing the low-lying  $J^\pi = 3/2^-, 5/2^-$  and  $7/2^-$  states.

$= 7/2^-$  and  $(7/2)^-$ , respectively [12]. In particular, the transition to the 2349 keV level has a  $\log f^0t = 6.04(7)$  that is very close to the value of an allowed GT transition [13]. In addition,  $\log f^1t = 7.38(8)$  for this transition is within the limit corresponding to a  $\Delta J = 0, 1$  transfer:  $\log f^1t_{\text{limit}} < 8.5$  [13]. Thus,  $\Delta J = 2$  is excluded for that transition leaving  $(5/2, 7/2, 9/2)^-$  as only possibility for the ground-state spin/parity. Similar argument, though weaker, is valid in the case of the transition to the 1023 keV level. These observations support the  $J^\pi = 5/2^-$  for the ground state of  $^{59}\text{Mn}$  instead of  $3/2^-$ . Additional support is given by the level systematics of the odd- $A$  Mn isotopes shown in fig. 4 [14]. The lowest  $3/2^-$  state between  $A = 51$  and 57 has been found at  $A = 57$  and lies at 850 keV. This is far above the low-energy  $5/2^-$ - and  $7/2^-$ -states that typically compete in forming the ground state in these nuclei. Based on the evidence given above we suggest  $J^\pi = 5/2^-$  for the ground state of  $^{59}\text{Mn}$ .

The observation of the 2348.9(9) keV and the non-observation of the 1137 keV  $\gamma$ -rays allow us to clarify the problem found in the case of the 2348.2(4) keV level [12]. Assignment of  $J^\pi = (7/2)^-$  is based on a (d,p)-reaction study with a relatively poor resolution resulting in a level energy of 2345(10) keV [6]. A level with an energy of 2348.2(4) keV was observed in the (n, $\gamma$ ) reaction work [7] and was shown to decay totally by 1137 keV  $\gamma$ -ray to the 1211 keV state with  $J^\pi = 1/2^-$ . These levels have been adopted to be the same so far with a comment [12] that two different levels very close to each other might be excited in the two reactions used in [6,7]. If  $J^\pi = 7/2^-$  for the level observed in [6] it would imply an  $M3$  transition to the 1211 keV level. This should be drastically hindered compared to a  $E2$  transition to the  $J^\pi = 3/2^-$  ground state of  $^{59}\text{Fe}$ , *i.e.* using the Weisskopf estimates  $\tau(M3, 1137 \text{ keV})/\tau(E2, 2348 \text{ keV}) \sim 2 \times 10^8$ . This is in contrast to previous findings and, in fact, the observation of the 2348.9(9) keV  $\gamma$ -ray in our spectrum is consistent with existence of two levels. Most likely the allowed  $\beta$ -decay populates the  $J^\pi = (7/2)^-$  state with an energy of

2348.9(9) keV which subsequently decays to the ground state of  $^{59}\text{Fe}$ . Thus we suggest that the 1137 keV  $\gamma$  transition, which is not observed in our spectrum, does not de-excite that level but is related to another one with possibly different  $J^\pi$ . We also note that fragmentation of the  $1f_{7/2}$  intruder strength has been considered to prevent the formation of shape coexistence in this region [15]. Based on the level energy considerations the observed state could be a candidate to contain a part of this strength [16].

## 5 Summary

Resonance Ionization Laser Ion Source has been employed for the production of  $^{59}\text{Mn}$  nuclei at the PSB-ISOLDE on-line mass separator facility at CERN. Based on the observed  $\beta$  transition rates and the level systematics the ground state of  $^{59}\text{Mn}$  is suggested to have  $J^\pi = 5/2^-$ . In addition, the  $\beta$ -decay populating the 2348.9(9) keV level in  $^{59}\text{Fe}$  could be used to solve a discrepancy between the previous reaction studies. This level is a good candidate to contain a part of the fragmented  $1f_{7/2}$  intruder strength considered to prevent the formation of shape coexistence in the region.

## References

1. N.G. Puttaswamy et al., Nucl. Phys. A **401**, 269 (1983).
2. R.C. Pardo et al., Phys. Rev. C **16**, 370 (1977).
3. E. Kashy et al., Phys. Rev. C **14**, 1773 (1976).
4. U. Bosch et al., Nucl. Phys. A **477**, 89 (1988).
5. D. Ward et al., Phys. Rev. C **45**, 2723 (1992).
6. T. Taylor and J.A. Cameron, Nucl. Phys. A **337**, 389 (1980).
7. R. Vennink et al., Nucl. Phys. A **344**, 421 (1980).
8. P. Lofy et al., *Proceedings of the International Conference "Nuclear Structure 2000", August 15-19, 2000, Michigan State University, East Lansing, MI, USA*, Nucl. Phys. A, **682** (2001).
9. V.I. Mishin et al., Nucl. Instr. and Meth. in Phys. Res. B **73**, 550 (1993).
10. V.N. Fedoseyev et al., Nucl. Instr. Meth. in Phys. Res. B **126**, 88 (1997).
11. M. Oinonen et al., Hyperfine Interact. **127**, 431 (2000).
12. C.M. Baglin, Nucl. Data Sheets **69**, 733 (1993).
13. S. Raman and N.B. Gove, Phys. Rev. C **7**, 1995 (1973).
14. R.B. Firestone et al., *Table of Isotopes* CD-ROM, Eight Edition Version 1.0, March 1996
15. K. Heyde et al., Phys. Rep. **102**, 291 (1983).
16. K. Heyde, private communication (2000).